



## Full length article

## Lipogels responsive to near-infrared light for the triggered release of therapeutic agents



Francisco Martín-Saavedra<sup>a,b,\*,1</sup>, Eduardo Ruiz-Hernández<sup>c,d,e,1</sup>, Clara Escudero-Duch<sup>b,a</sup>, Martín Prieto<sup>f,a</sup>, Manuel Arruebo<sup>f,a</sup>, Negar Sadeghi<sup>g</sup>, Roel Deckers<sup>h</sup>, Gert Storm<sup>g</sup>, Wim E. Hennink<sup>g</sup>, Jesús Santamaría<sup>f,a</sup>, Nuria Vilaboa<sup>b,a,\*</sup>

<sup>a</sup> CIBER de Bioingeniería, Biomateriales y Nanomedicina, CIBER-BBN, Spain

<sup>b</sup> University Hospital La Paz-IdiPAZ, Paseo de la Castellana 261, 28046 Madrid, Spain

<sup>c</sup> School of Pharmacy and Pharmaceutical Sciences, Trinity College Dublin, The University of Dublin, College Green, Dublin 2, Ireland

<sup>d</sup> Tissue Engineering Research Group, Dept. of Anatomy, Royal College of Surgeons in Ireland, 123 St Stephen's Green, Dublin 2, Ireland

<sup>e</sup> Advanced Materials and Bioengineering Research (AMBER) Centre, CRANN Institute, Trinity College Dublin, Dublin 2, Ireland

<sup>f</sup> Aragon Institute of Nanoscience (INA), University of Zaragoza, Campus Río Ebro, Edificio I+D, C/Mariano Esquillor s/n, 50.018 Zaragoza, Spain

<sup>g</sup> Department of Pharmaceutics, Utrecht Institute for Pharmaceutical Sciences, Utrecht University, PO BOX 80082, 3508 TB Utrecht, The Netherlands

<sup>h</sup> Imaging Division, University Medical Center Utrecht, Heidelberglaan 100, 3584 CX Utrecht, The Netherlands

## ARTICLE INFO

## Article history:

Received 11 April 2017

Received in revised form 19 July 2017

Accepted 7 August 2017

Available online 8 August 2017

## Keywords:

Hydrogel

Thermosensitive liposome

Optical hyperthermia

Near infrared

Photoabsorber

## ABSTRACT

Here we report a composite system based on fibrin hydrogels that incorporate in their structure near-infrared (NIR) responsive nanomaterials and thermosensitive liposomes (TSL). Polymerized fibrin networks entrap simultaneously gold-based nanoparticles (NPs) capable of transducing NIR photon energy into heat, and lysolipid-incorporated TSL (LTSL) loaded with doxorubicin hydrochloride (DOX). NIR irradiation of the resulting hydrogels (referred to as “lipogels”) with 808 nm laser light increased the temperature of the illuminated areas, leading to the release of the liposomal cargo. Levels of DOX that release from the “smart” composites were dependent on the concentration of NIR nanotransducers loaded in the lipogel, the intensity of the electromagnetic energy deposited and the irradiation regime. Released DOX retained its bioactivity, as shown in cultures of epithelial carcinoma cells. Finally, the developed drug delivery platform was refined by using NIR-photoabsorbers based on copper sulfide NPs to generate completely biodegradable composites as well as through the incorporation of cholesterol (Ch) in LTSL formulation, which lessens leakiness of the liposomal cargo at physiological temperature. This remotely controlled system may suit well for those therapies that require precise control over the dose of delivered drug in a defined spatiotemporal framework.

## Statement of Significance

Hydrogels composed of fibrin embedding nanoparticles responsive to near infrared (NIR) energy and thermosensitive liposomes loaded with doxorubicin hydrochloride (DOX), were prepared by *in situ* polymerization. NIR-light irradiation of these constructs, referred to as “NIR responsive lipogels”, results in the controlled release of DOX to the surrounding medium. This technology may use fully degradable components and can preserve the bioactivity of liposomal cargo after remote triggering to finely regulate the dose and bioavailability of delivered payloads. NIR responsive lipogels technology overcomes the limitations of drug release systems based on the combination of liposomes and degradable polymeric materials, which in many cases lead to insufficient release at therapy onset or to overdose during high degradation period.

© 2017 Acta Materialia Inc. Published by Elsevier Ltd. All rights reserved.

\* Corresponding authors at: University Hospital La Paz-IdiPAZ, 28046 Madrid, Spain.

E-mail addresses: [fco.martin.saavedra@gmail.com](mailto:fco.martin.saavedra@gmail.com) (F. Martín-Saavedra), [ruizhere@tcd.ie](mailto:ruizhere@tcd.ie) (E. Ruiz-Hernández), [claraescudero Duch@gmail.com](mailto:claraescudero Duch@gmail.com) (C. Escudero-Duch), [martinprieto@fraga@gmail.com](mailto:martinprieto@fraga@gmail.com) (M. Prieto), [arruebom@unizar.es](mailto:arruebom@unizar.es) (M. Arruebo), [n.sadeghi@uu.nl](mailto:n.sadeghi@uu.nl) (N. Sadeghi), [deckers-2@umcutrecht.nl](mailto:deckers-2@umcutrecht.nl) (R. Deckers), [g.storm@uu.nl](mailto:g.storm@uu.nl) (G. Storm), [w.e.hennink@uu.nl](mailto:w.e.hennink@uu.nl) (W.E. Hennink), [jesus.santamaria@unizar.es](mailto:jesus.santamaria@unizar.es) (J. Santamaría), [nuria.vilaboa@salud.madrid.org](mailto:nuria.vilaboa@salud.madrid.org) (N. Vilaboa).

<sup>1</sup> These authors contributed equally.

## 1. Introduction

Hydrogels and other polymer-based carriers have emerged as promising systems to provide reservoirs for pharmaceuticals acting in a variety of anatomical regions. Highly biodegradable and biocompatible fibrin gels, obtained by thrombin-catalyzed polymerization of fibrinogen, have been used since last century with remarkable success as post-surgery sealants and stand out for their potential as controlled delivery systems of various pharmaceutical agents [1]. After addition of thrombin to a fibrinogen solution, fibrin networks can be prepared in the form of macroscopic gels, films, threads, microbeads or nanoparticles. The final properties of the gels, including porosity and degradability, can be tailored by the process and formulation parameters [2]. The release of drugs from fibrin gels occurs via diffusion once the pores in the network are bigger than the hydrodynamic size of the entrapped therapeutics [3]. Moreover it has been shown that the release can be modulated by entrapment of protease inhibitors in the protein matrix that slow down the *in vivo* degradation, by crosslinking with bifunctional reagents that enhance the retention of the therapeutic agents in the protein network or by covalent linking of the payloads to the matrix [4–6]. Entrapment of drug-loaded nanoparticles, e.g. liposomes, can remarkably lower the release rates of water-soluble therapeutics that readily diffuse out from fibrin gels [7,8].

Liposomes are sphere-shaped, unilamellar or multilamellar vesicles typically made from phospholipids. Hydrophobic drugs can be solubilized in the lipid bilayer while more hydrophilic drugs can be loaded in the aqueous core of liposomes. Pharmaceutical agents retained by liposomes become bioavailable only after being released. Most attempts to use liposomes as drug delivery vehicles are based on considering liposomes as entities that circulate in the blood, being taken up by certain cells or tissues to slowly release their therapeutic cargo as they degrade [9–11]. Optimization of the release rate of entrapped drug is essential to control local drug concentration and increase the therapeutic outcome of liposomes [12,13]. Several drug delivery systems aiming sustained release of therapeutic peptides, proteins or drugs from liposomes have been proposed, including their encapsulation in fibrin networks [7,8,10,11]. Also, triggering modalities for site-specific release of therapeutics have been developed to improve the therapeutic efficacy of liposomal formulations. These strategies include local triggers which are specific to target sites (e.g., pH and enzymes) and remote triggers (e.g., temperature, ultrasound, magnetic field, radiofrequency and light) through the use of specific lipid compositions and coatings [14–17]. Among the latter approaches, heat-based delivery appears to be the most promising to date [18]. TSL are special formulations capable of releasing encapsulated cargos in response to an increase of temperature, whilst preventing premature leakage at physiological temperature [19]. Incorporation of lysolipids, phospholipids with one hydrocarbon chain, in the formulation of TSL can lower the phase transition temperature of the lipid bilayer to the mild hyperthermia range [20–22]. Upon heating, lysolipids create and stabilize water-filled pores along liquid-solid boundaries formed in the lipid bilayer of liposomes, enhancing its permeability [18]. An example of LTSL is ThermoDox<sup>®</sup>, a heat-activated liposomal formulation of doxorubicin that upon intravenous administration releases the entrapped drug at temperatures above 40 °C. This formulation, the first and only thermosensitive liposome formulation to reach clinical development to date [23], is currently being evaluated in combination with radiofrequency thermal ablation for the treatment of hepatocellular carcinoma in the OPTIMA trial [24], a clinical phase III trial based on the promising findings obtained from *post-hoc* analysis of the HEAT trial [25]. A major drawback of systemically adminis-

tered liposomes, as ThermoDox<sup>®</sup>, is their poor and inhomogeneous distribution at distances away from the tumor vasculature which can compromise clinical outcomes. Furthermore, radiofrequency energy is difficult to focus on a discrete target site. These limitations may be circumvented by technologies that allow direct disposal of thermosensitive liposomes in the tumor region and that employ focusable sources of heat to trigger drug release.

In the present work, we exploit the ability of fibrin hydrogels to incorporate in their structure inorganic photoabsorbers such as hollow gold nanoparticles (HGNP) [26] or copper sulfide nanoparticles (CuSNP) [27] during gelation [28]. Both NPs exhibit strong light absorption at near-infrared (NIR) wavelengths (650–1050 nm) and can convert light energy into thermal energy through localized surface plasmon resonance, and in the case of CuSNP, also through the excitation of direct (band-to-band) or indirect electronic transitions due to their semiconductor character [29]. We hypothesized that incorporating NIR nanotransducers (NIR-NT) in fibrin matrices that include DOX-loaded LTSL (LTSL-DOX), referred to as “lipogels” [30,31], may result in an advanced drug delivery platform exogenously regulated by NIR electromagnetic energy, which has its maximum depth of penetration in biological tissue (Fig. 1).

## 2. Materials and methods

### 2.1. Chemical reagents

The phospholipids 1,2-Dipalmitoyl-*sn*-glycero-3-phosphocholine (DPPC), 1,2-Distearoyl-*sn*-glycero-3-phosphocholine (DSPC), and 1,2-Distearoyl-*sn*-glycero-3-phosphoethanolamine-N-poly(ethylene glycol)-2000 (DSPE-PEG2000) were provided by Lipoid (Ludwigshafen, Germany). Monostearoylphosphatidylcholine (MSPC) was purchased from Avanti Polar Inc (Alabaster, AL, USA). Other chemical reagents were purchased from Sigma Aldrich unless otherwise specified.

### 2.2. DOX-loaded liposomes

LTSL or cholesterol-containing LTSL (LTSL-Ch) were prepared as follows. DPPC:MSPC:DSPE-PEG2000 or DPPC:MSPC:DSPE-PEG2000:Ch were dissolved in chloroform in a molar ratio of 86:10:4 or 81.7:9.5:3.8:5, respectively. A lipid film was formed in a rotavapor under vacuum at 40 °C. Residual solvent was removed by flushing the film with nitrogen gas for 1 h. Liposomes were prepared by hydrating the film with 240 mM ammonium sulfate buffer (pH 5.5) at 60 °C, aiming to a final lipid concentration of 25 mg mL<sup>-1</sup>. Polycarbonate membrane filters (650, 200 and 100 nm) were employed to extrude the resulting liposomes at 60 °C. Loading of DOX into liposomes was performed using the pH gradient loading method as previously described [32,33], with initial DOX-to-lipid ratio of 1:20 (mol:mol). Briefly, extravesicular buffer was exchanged using 10 kDa cut-off membranes with dialyzing medium HBS pH 7.4 (20 mM HEPES, 150 mM NaCl) at 500 volumes for 1 volume of liposomal dispersion in three repeated cycles, establishing the gradient. Liposomes were loaded with DOX by incubation at 37 °C for 1 h. Unencapsulated DOX molecules were removed using Sephadex G-25 gel filtration resins. LTSL-DOX or LTSL-Ch-DOX were suspended in HBS pH 7.4 and stored at 4 °C. Liposome size was measured by dynamic light scattering (DLS) using a Malvern 4700 compact goniometer (Malvern GmbH, Germany). Calorimetric studies were carried out in a Mettler-Toledo differential scanning calorimeter with a high-sensitivity sensor. Scans were performed in a range of 20–50 °C and recorded

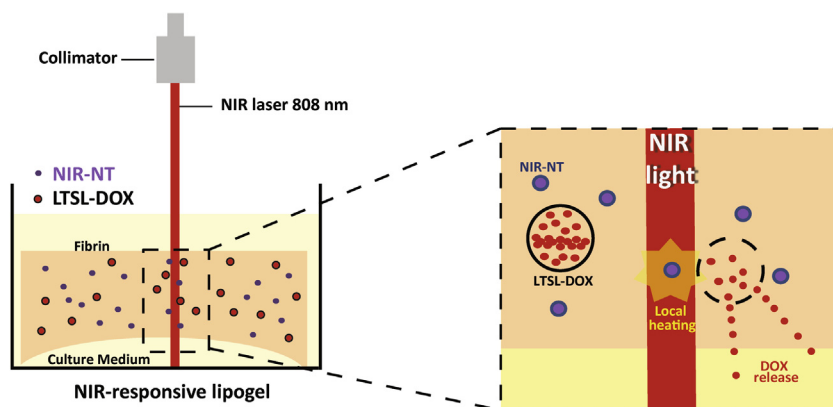


**Fig. 1.** Schematic illustration of the experimental procedure to trigger DOX release from lipogels, harboring LTSL-DOX and NIR-NT, upon irradiation with a collimated laser emitting at 808 nm.

at a rate of 0.5 °C/min. A scan made with the reference sample (HBS buffer) was employed as basal line for the calorimetric assays.

### 2.3. Encapsulation capability of LTSL and DOX release kinetics

Encapsulation efficiency and drug release were determined by taking advantage of the self-quenching fluorescent properties of DOX [34]. DOX precipitates encapsulated in liposomes are in close proximity to each other and do not produce appreciable fluorescence signal. However, when released into surrounding media and diluted, DOX fluorescence is restored providing a method of quantifying release. Fluorescence intensity of DOX encapsulated into LTSL was measured following lysis with 2% Triton X-100, by spectrofluorometry (Biotek, Winooski, VT, USA) at excitation and emission wavelengths of 485 and 600 nm, respectively. Encapsulation efficiency of three different batches of LTSL-DOX and one batch of LTSL-Ch-DOX were  $96 \pm 3\%$  and  $87\%$ , respectively. The *in vitro* release kinetics of DOX from LTSL-DOX was monitored by fluorometry after dilution of the liposomal sample in HBS pH 7.4 and incubation at 37–43 °C in a thermostated water bath.

### 2.4. NIR nanotransducers

HGNP, with an average diameter of  $\sim 36$  nm and a wall thickness of  $\sim 8$  nm, exhibiting a maximum of absorbance at 780 nm, were synthesized as described elsewhere [26]. CuSNP with an average diameter of  $\sim 70$  nm and exhibiting a strong optical absorption in the 650–1100 nm range, were synthesized according to a previously reported method [27].

### 2.5. Preparation of NIR-responsive lipogels and DOX release kinetics

Bovine fibrinogen (fbg; Sigma-Aldrich) was dissolved in ice-cold Dulbecco's modified Eagles's medium (DMEM; Cultek, Madrid, Spain) at a concentration of  $40 \text{ mg mL}^{-1}$  of clottable protein. HGNP or CuSNP were diluted at  $2 \text{ mg mL}^{-1}$  in double-distilled water and then sonicated at maximum power for 10 min in a water bath sonicator (Branson 12, Branson Ultrasonidos S.A.E., Barcelona, Spain). NPs were added to ice-cold DMEM at  $0.1$ – $0.5 \text{ mg mL}^{-1}$  and thoroughly vortexed to obtain a homogenous particle suspension. A 0.1 volume of NP-containing suspensions and 0.8 volume of DMEM containing  $0.05 \text{ mg mL}^{-1}$  LTSL-DOX were added to 1 volume of dissolved fbg. Finally, 0.1 volume of  $40 \text{ U mL}^{-1}$  bovine thrombin (Sigma-Aldrich) dissolved in ice-cold DMEM was added to the resulting mixture. After homogenization of components by pipetting, the suspension was distributed to multiwell tissue culture plates (Sigma-Aldrich) pretreated with heat-inactivated fetal

bovine serum (FBSi, GE Healthcare Life Sciences, Madrid, Spain). Final volumes of suspension were 1 mL for 12-well plates (serial NIR-irradiation experiments) or 0.25 mL for 48-well plates (other experiments). Suspensions were allowed to clot in a humidified 5%  $\text{CO}_2$  atmosphere at 37 °C (37 °C/5%  $\text{CO}_2$ ) for 30 min. The hydrogels were allowed to equilibrate with 1 volume of DMEM containing 20% FBSi (DMEM-20%FBSi) for 1 h at 37 °C/5%  $\text{CO}_2$ . Hydrogels were thoroughly washed with 10 volumes of PBS 2 times, immersed in 40 volumes of PBS and incubated at 37 °C/5%  $\text{CO}_2$  for 16 h prior heat, light or chemical treatment. To determine total amount of DOX in the lipogels, the samples were immersed in 10% Triton X-100 and incubated at room temperature (RT) for 24 h under constant agitation in an orbital shaker set at 300 rpm. To characterize the kinetics of DOX release from the matrices, fibrin hydrogels with a final volume of 0.25 mL were allowed to clot for 30 min in the presence of  $0.06 \text{ mg mL}^{-1}$  DOX at 37 °C/5%  $\text{CO}_2$ , and then supplemented with 0.25 mL of DMEM-20% FBSi and further incubated for 30 min. Media were discarded and hydrogels were incubated with PBS or cell growth medium, composed of DMEM supplemented with 10% (v/v) FBSi and  $10 \text{ UI mL}^{-1}$  of penicillin and streptomycin (Thermo Fisher Scientific, Madrid, Spain), for 2 h. During this period, the aqueous solutions were collected every 10 min and replaced with an equal volume of the corresponding fresh solution. Concentrations of DOX in the aqueous solutions were estimated by fluorometry as described in Section 2.3, using known amounts of DOX dissolved in cell growth medium that served as reference for absolute quantification (Supplementary Fig. S1). Higuchi model for the rate of drug release from matrix devices [35] fitted well with the kinetics of DOX release, resulting in a correlation coefficient  $>0.99$  (Supplementary Fig. S2).

### 2.6. Microscopy

Encapsulated DOX inside liposomes was visualized using transmission electron microscopy (TEM) techniques. To obtain cryo-TEM images, a thin liquid film of the sample placed on a microperforated copper grid was frozen in liquid ethane and prepared for imaging in a chamber cooled with liquid nitrogen attached to a Tecnai T12 TEM microscope. TEM images of LTSL-DOX after filtration through a  $0.22 \mu\text{m}$  polyethersulfone (PES) membrane were obtained after placing a thin layer of the liposomal sample on a 400-mesh carbon-coated copper grid, fixing with 2.5% glutaraldehyde, contrasting with 2% uranyl acetate and embedding in 0.13% methyl cellulose. To characterize NIR-responsive lipogels by TEM, the above-described components for preparing fibrin-based hydrogels were mixed and then diluted ten-fold in PBS. A drop of this

dilution was placed on a 400-mesh carbon-coated copper grid and allowed to polymerize for 5 min at 37 °C. DOX-loaded liposomes and lipogels were visualized in a JEM 1010 electron microscope (JEOL, Peabody, MA, USA).

DOX encapsulated in LTSL loaded in NIR-responsive lipogels was visualized by biomapping using a confocal laser scanning microscope (CLSM, Leica TCS-SP5 AOBS, Leica microsystems, Heidelberg, Germany). Lipogel samples were excited with an argon laser at 488 nm and emission was collected between 490 and 580 nm. A  $3872 \times 1456$  pixels square of  $11.72 \times 4.41$  mm covering the lipogel along a depth of 500  $\mu$ m distributed in 10 Z-stacks was acquired with a 10X, 0.5 NA dry objective. CLSM images were analyzed and reconstructed using Leica software LAS AF, version 2.6.0.7266.

### 2.7. NIR laser irradiation of lipogels to trigger DOX release

The NIR irradiation set-up consisted of an 808 nm laser module operating in continuous wave mode (MXL-III(FC) model, Changchun New Industries Optoelectronics Technology Co., Ltd., Changchun, China), coupled to an optical fiber of 400  $\mu$ m of diameter and a fixed focus collimator (Thorlabs, Newton, NJ, USA). Collimated fiber optic was attached to a micropositioning system and placed in a thermostatically-controlled chamber (Model Stuart SI60D, Fisher Scientific, Afora, Madrid, Spain) to establish the environmental temperature at 37 °C, as previously described [28]. Laser power output was measured by a silicon photodiode sensor (Model PD300-3 W, Ophir Laser Measurement Group, Logan UT, USA). A VRC4 IR detector card (Thorlabs) was used to determine that irradiation spot had  $6.32 \pm 0.14$  mm of diameter at the target site. Changes in surface temperature of lipogels were monitored by IR thermography using a camera for thermal imaging (875-2i model, Instrumentos Testo S.A., Madrid, Spain). Lipogels with a final volume of 0.25 or 1 mL were irradiated after immersion in 0.25 or 1 mL of fresh cell growth medium, respectively. Quantification of the superficial area from which DOX was discharged after illumination of the lipogel was calculated using Fiji software [36].

### 2.8. Cell viability assays

Human cervical cancer cells (HeLa, ATCC CCL-2) were cultured in cell growth medium. Cells were incubated at 37 °C/5% CO<sub>2</sub> inside a humidified incubator. HeLa cells were seeded in 96-well plates, subsequently cultured for 24 h and then further incubated up to 24 h in cell growth medium conditioned or not by lipogels. Cell viability was assessed using the alamarBlue reagent (Biosource, Nivelles, Belgium), which incorporates a redox indicator, resazurin, that in response to metabolic activity is reduced to the strongly fluorescent resorufin. After washing with PBS, the cells were incubated in cell growth medium containing 10% alamarBlue dye for 4 h. Media were collected and after laser excitation at 530 nm, 590 nm emitted fluorescence was quantified using a spectrofluorimeter Synergy4 (BioTek). As a control of DOX cytotoxicity, viability of cells treated for 24 h with DOX dissolved in cell growth medium was measured (Supplementary Fig. S3).

### 2.9. Statistics

Data are presented as means  $\pm$  standard deviation (SD) of at least three independent experiments. For statistical analysis, one-way ANOVA followed by Dunnett's multiple comparisons test was performed using GraphPad Prism Version 6.00. The criterion for significance in statistical analyses was set at  $p \leq 0.05$ .

## 3. Results

### 3.1. Characterization of LTSL-DOX

Fig. 2A shows cryo-TEM images of LTSL-DOX prepared by the lipid film hydration and extrusion method and then loaded with the drug by a transmembrane proton gradient technique. As previously described for DOX-loaded liposomes using citrate-gradient [37], accumulation of the drug into the acidic interior of the liposomes loaded with 240 mM ammonium sulfate buffer (pH 5.5) led to the generation of linear, circular and curved bundles of DOX fibers that change liposomal shape, resulting in characteristic “coffee bean” structures, with no significant perturbation of the vesicle membrane [38]. DLS analysis of LTSL-DOX sample determined an average size of 159 nm and a polydispersity index of 0.073 (Fig. 2B). Differential scanning calorimetry (DSC) analysis of LTSL-DOX evidenced two phase transition peaks, namely a low enthalpic pre-transition at around 36.7 °C and a main endothermic transition at 40.5 °C (Fig. 2C). Triggered DOX release from LTSL-DOX suspended in water occurs at 40 °C (Supplementary Fig. S4), while drug release detected at 37 °C was marginal, even when incubation was prolonged to 20 min (Fig. 2D). In contrast, heating at 42 °C for 5 min resulted in the release of the 90% of the loaded drug.

### 3.2. Photothermal characterization of fibrin-based hydrogels incorporating HGNP and LTSL-DOX

LTSL-DOX suspension was diluted in DMEM and then filtered through a PES membrane to remove aggregates and increase the uniformity of liposomal sample (Fig. 3A). Subsequently, LTSL-DOX were incorporated together with HGNP into fibrin gels through *in situ* thrombin-catalyzed polymerization of fibrinogen. TEM imaging of the resulting lipogel showed the entrapment of LTSL-DOX in the fibrin matrix incorporating HGNP (Fig. 3B). IR-thermal imaging of lipogels irradiated with a collimated laser diode emitting light with a wavelength of 808 nm showed a rapid temperature increase of the HGNP-containing matrices (Fig. 3C). The temperature of the hydrogels increased as a function of the HGNP concentration in the fibrin network. After 5 min of exposure to NIR laser, the temperature at the surface of the lipogels containing 0.01 mg mL<sup>-1</sup> HGNP raised  $4.2 \pm 0.9$  °C at the spot at which the laser beam was focused. Same irradiation conditions led to an increase of  $25.4 \pm 2.3$  °C for lipogels loaded with 0.05 mg mL<sup>-1</sup> HGNP (graph in Fig. 3C). As can be observed in the photographs, irradiated lipogels containing 0.02–0.05 mg mL<sup>-1</sup> HGNP showed a discrete unstained region on their surfaces. The shape of this region was a circle, concentric to the focus of the laser beam, which area increased with the concentration of HGNP incorporated in the lipogel (Table 1). Interestingly, the unstained region of lipogels loaded with 0.05 mg mL<sup>-1</sup> HGNP showed an internal darker spot likely due to excessive heat that leads to conformational changes of the fibrin matrix. Fluorescence imaging of NIR-responsive lipogels by CLSM biomapping revealed the fading of DOX fluorescence in a region concentric to the site where the laser was focused, which extended over the entire Z axis of the lipogel (Fig. 3D).

DOX release from lipogels incubated for 1 h at 37 °C could not be detected by fluorometry under the employed experimental conditions. To determine whether mild hyperthermia effectively induces drug release from LTSL-DOX lipogels, the composites were heated at 42 °C for 1 h in a water bath. About 30% of the loaded amount of DOX was released as a result of the thermal treatment (Fig. 4A), leading to loss of the red color, provided by DOX, in the composites (Fig. 4A, photographs). HGNP embedded in the lipogel did not significantly alter the levels of released DOX after heat



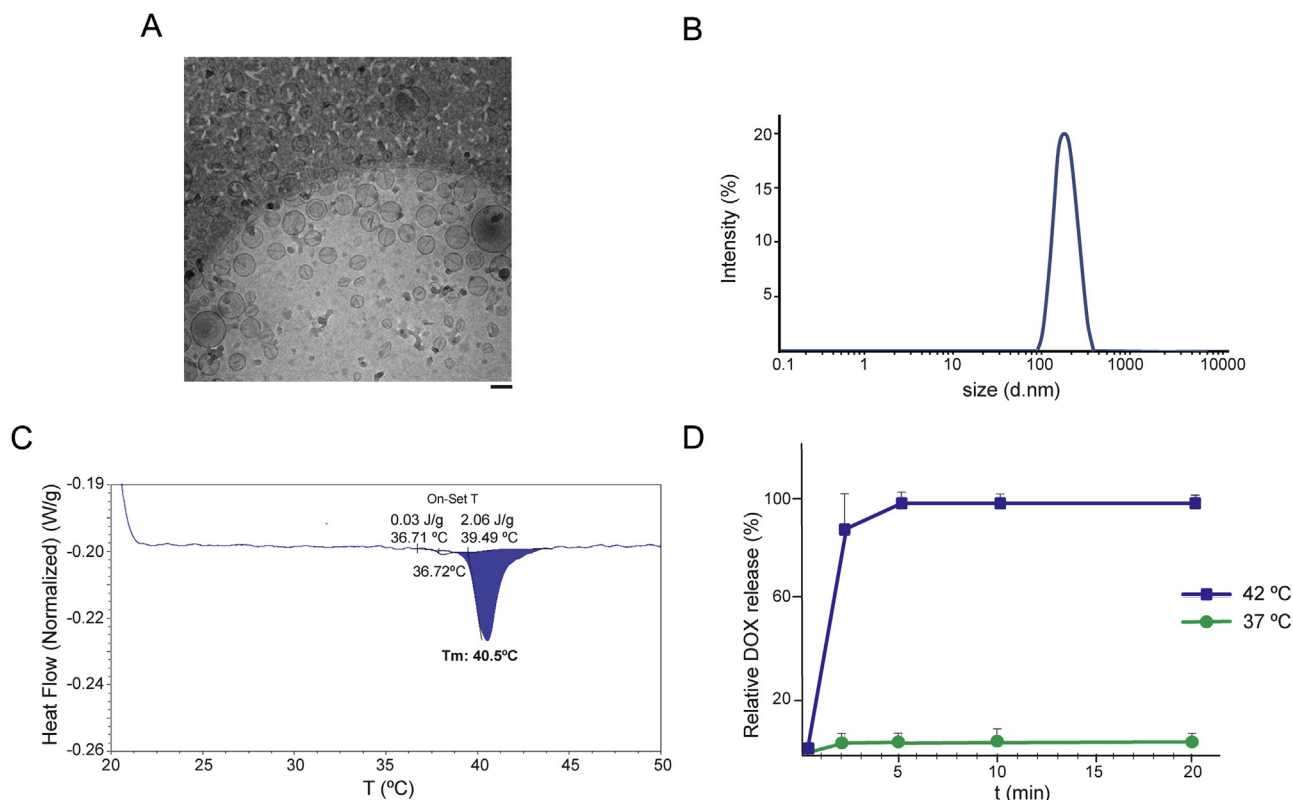


**Fig. 2.** Characterization of LTSL-DOX. (A) Cryo-TEM image of LTSL-DOX after drug loading at drug-to-lipid ratio of 1:20 (mol:mol). Image is representative of the entire sample. (B) Particle size distribution of synthesized LTSL-DOX. (C) DSC scan of LTSL-DOX sample. (D) Cumulative DOX release in the supernatant of LTSL-DOX suspensions incubated for the indicated time at 37 or 42 °C. Mean and SD values are relative to the average drug level in samples treated at 42 °C for 20 min, which was given an arbitrary value of 100. Scale bar = 100 nm.

treatment in the water bath. Fig. 4B shows the relative amount of drug that released from NIR-responsive lipogels after irradiation at  $44 \text{ mW mm}^{-2}$  for 10 min. NIR-treatment of lipogels containing  $0.03 \text{ mg mL}^{-1}$  HGPN resulted in a DOX release similar to that induced in lipogels devoid of NIR-NT that were heated in a water bath. DOX concentrations in the conditioned media were estimated at  $3.27 \pm 0.29$  and  $3.48 \pm 0.37 \mu\text{g mL}^{-1}$ , respectively. Interestingly, the extent of DOX release was dependent on the concentration of HGPN in the lipogels. Thus, concentration of DOX in media conditioned by irradiated lipogels loaded with  $0.01 \text{ mg mL}^{-1}$  HGPN was  $0.68 \pm 0.31 \mu\text{g mL}^{-1}$ , 5-fold lower than when lipogels loaded with  $0.03 \text{ mg mL}^{-1}$  HGPN were irradiated with same intensity of energy. To study the bioactivity of DOX released from lipogels, HeLa cells were incubated in cell growth media conditioned by NIR-irradiated constructs incorporating LTSL-DOX. Media conditioned by NIR-treated lipogels loaded with  $0.03 \text{ mg mL}^{-1}$  HGPN reduced cell viability to about 10%, similarly to media collected from HGPN-lacking lipogels heated at 42 °C for 1 h (Fig. 4B). After NIR treatment, the released drug from LTSL-DOX lipogels containing  $0.01 \text{ mg mL}^{-1}$  HGPN reduced the viability of cell cultures by about 35%. Metabolic activity of HeLa cells treated with media conditioned by lipogels incubated at 37 °C for 1 h was similar to that measured in cells treated with fresh medium.

To investigate whether spatiotemporal control of DOX release can be achieved, NIR-responsive lipogels were irradiated at different spots, for 5 or 10 min per location. We found that the region of DOX discharge in lipogels containing  $0.02 \text{ mg mL}^{-1}$  HGPN increased with the time of laser exposure as well as with the number of irradiations performed at discrete sites (Fig. 5A). The highest release of DOX was obtained after 3 serial irradiations of 10 min

each (Fig. 5B). Fewer irradiations or shortening their duration resulted in lower drug release. Loss of HeLa cell viability correlated well with the concentration of DOX released into the culture medium (Fig. 5B). Collectively, this set of assays demonstrated that, by modulating the concentration of HGPN or the NIR irradiation regime, the extent of DOX release from NIR-responsive lipogels can be finely tuned.

### 3.3. Refining drug delivery from NIR-responsive lipogels

Although the results shown indicate that fibrin hydrogels containing LTSL-DOX and HGPN are efficient systems for NIR-controlled local drug delivery, there are some aspects that should be taken into account. Thus, although only a small leakage occurs at 37 °C, this may lead to toxicity problems prior to heat activation. Another concern relates to the use of gold-based NPs for photonic transduction as there is a serious lack of information concerning their effects on human health. Although HGPN cytotoxicity is very low [26,28], their bioinert character prevents *in vivo* degradation and therefore hinders their potential excretion from the body by hepatobiliary or renal mechanisms [39]. This latter feature may be an obstacle for the implementation of NIR-responsive lipogels technology in the clinical scenario.

We aimed to minimize cell toxicity due to cargo leakiness of LTSL-DOX at normal body temperature range. The stability of the vesicles at 37 °C was optimized by incorporating 5% Ch in their formulation. It is well known that this steroid introduces a significant variation in liposomal structures through stoutness control by increasing the packing of phospholipids [40]. LTSL-Ch prepared using the lipid film hydration and extrusion method were loaded with DOX using same drug-to-lipid ratio that employed for the

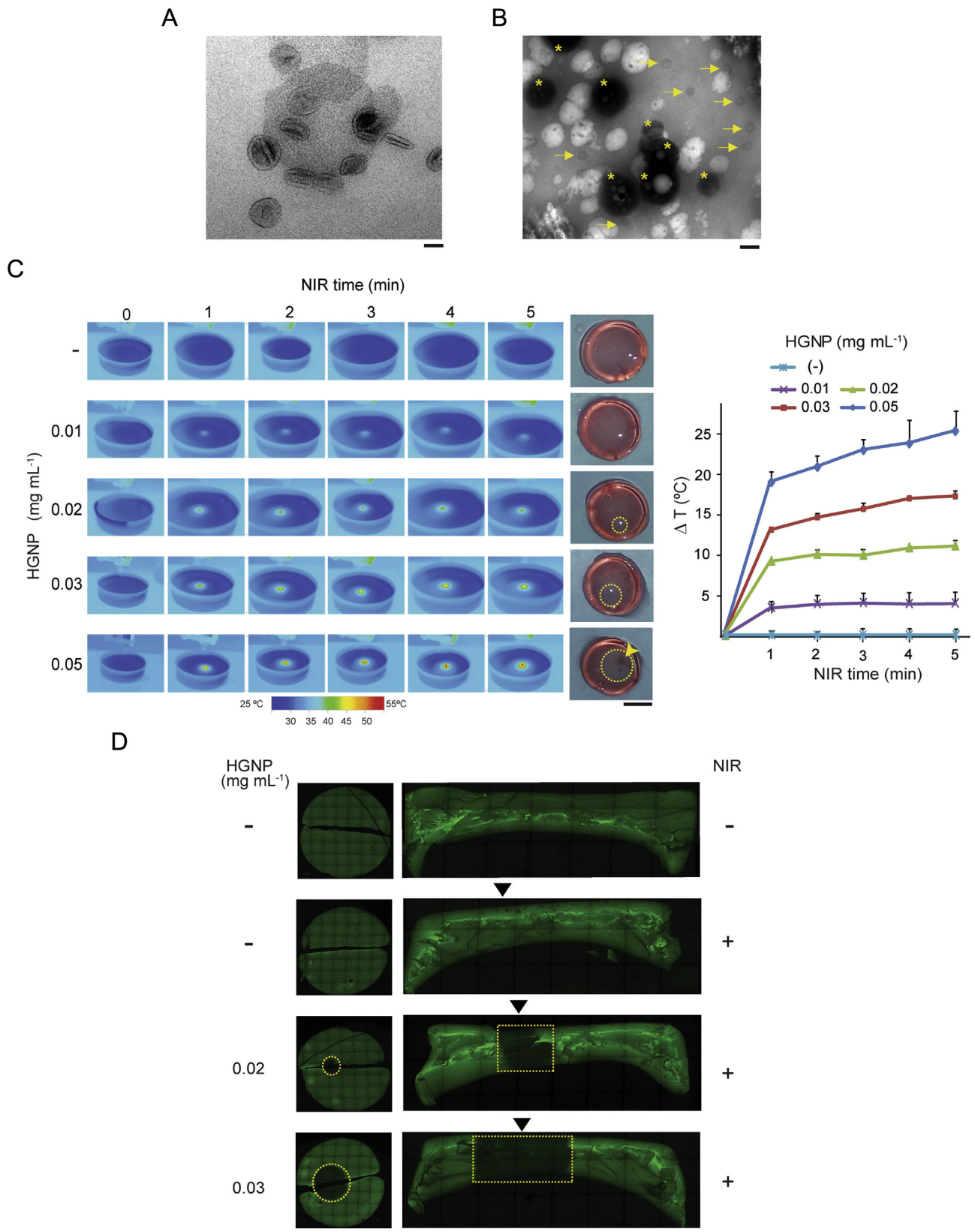


**Fig. 3.** Characterization of NIR-responsive lipogels. TEM image of LTSL-DOX sample filtered through a PES membrane (A) or entrapped in a fibrin matrix containing 0.02 mg mL<sup>-1</sup> HGNP (B). Asterisks indicate LTSL-DOX, arrows indicate HGNP. (C) Lipogels, containing the indicated concentrations of HGNP or not containing HGNP (-), were irradiated with NIR laser at 44 mW mm<sup>-2</sup> for the indicated times and monitored by IR thermography. Photographs show the surface of NIR-responsive lipogels after NIR energy treatment. Dashed circles indicate the region of lipogels where DOX was discharged. Arrow indicates the lipogel region where the conformation change of protein matrix is macroscopically visible. The graph shows the maximum temperature rise detected during NIR irradiation. (D) CLSM-biomapping images of top and cross-sectional views of lipogels containing the indicated doses of HGNP, NIR-irradiated for 10 min at 44 mW mm<sup>-2</sup> (NIR+) or not irradiated (NIR-). Arrows indicate the point of laser incidence on lipogel. Areas marked with dashed lines indicate the lipogel regions where DOX fluorescence fades. Scale bar = 100 nm (TEM images), 5 mm (photographs), 2 mm and 1 mm (top and cross-sectional views of CLSM images, respectively).

**Table 1**  
Quantification of DOX discharge area in lipogels.

[NPs] mg mL <sup>-1</sup>	HGNP	CuSNP
0.05	37.83 ± 0.44	35.22 ± 0.56*
0.03	19.67 ± 0.75	17.59 ± 0.63*
0.02	11.93 ± 0.61	10.75 ± 0.73
0.01	N.D.	N.D.
–	N.D.	N.D.

The data are expressed as mm<sup>2</sup> of surface area. Each value represents the mean ± SD of three independent experiments. N.D.: not detected. \* p < 0.05 compared to lipogels loaded with HGNP.

preparation of LTSL-DOX. DSC analysis of LTSL-Ch-DOX revealed a main endothermic transition at 40.4 °C (Fig. 6A). These vesicles lacked the low enthalpic pre-transition peak around ~37 °C displayed by LTSL-DOX (Fig. 2C), and thus DOX levels detected in the conditioned media of lipogels loaded with LTSL-Ch-DOX and incubated at 37 °C for 24 or 96 h were significantly lower as compared to the formulation without Ch (Fig. 6B). Interestingly, LTSL-Ch-DOX lipogels exposed to a non-focused heating source as well as after NIR-irradiation were more efficient in releasing the loaded drug than their counterparts based in LTSL-DOX (Fig. 6B). Taken

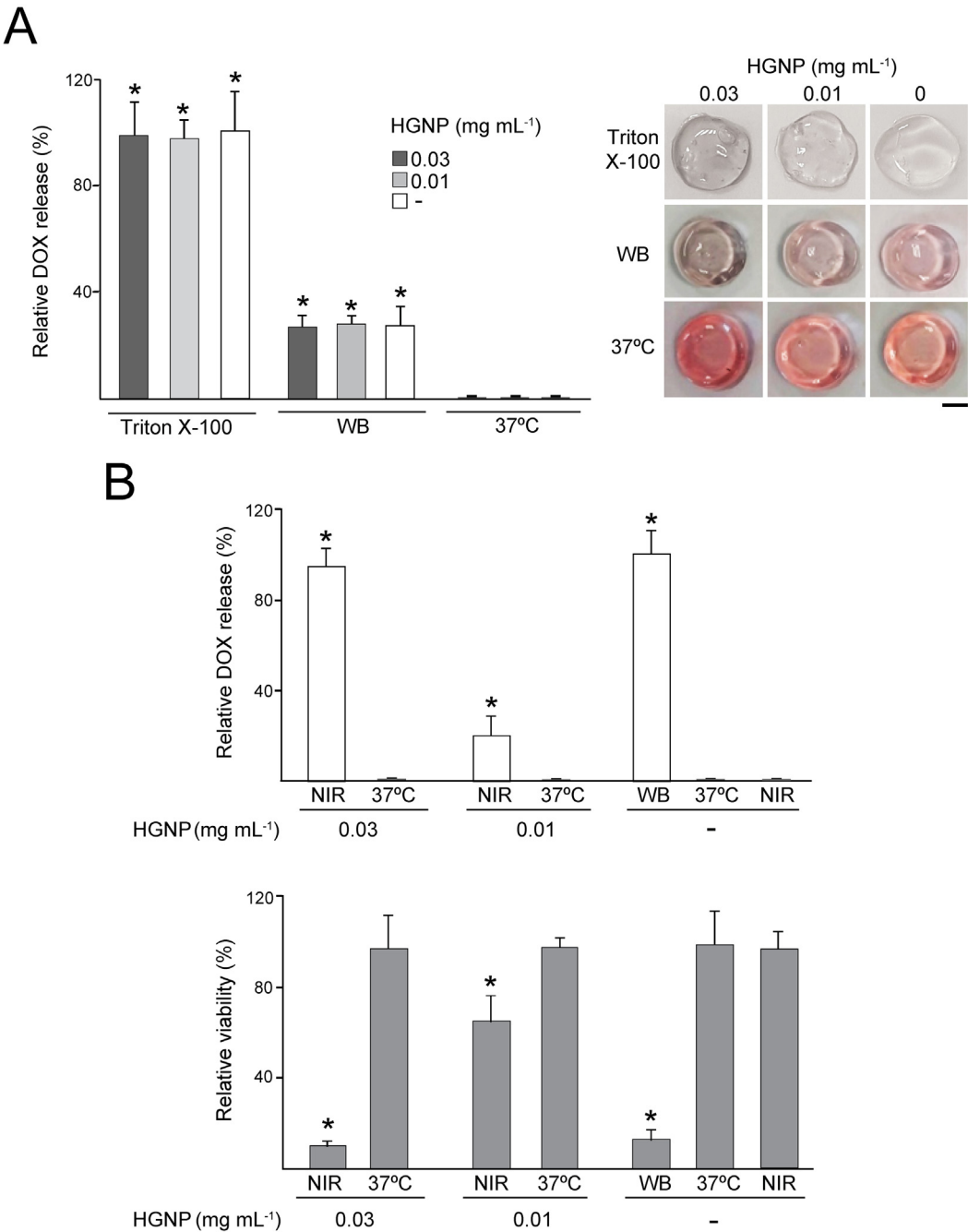


**Fig. 4.** Triggering of drug release from NIR-responsive lipogels. (A) DOX release into the culture media of LTSL-DOX lipogels containing the indicated doses of HGNP or not containing HGNP (–), after incubation at 42 °C (water bath, WB) or incubation at 37 °C/5% CO<sub>2</sub> (37 °C) for 1 h. Complete disintegration of LTSL-DOX encapsulated within lipogels was achieved after treatment with 10% Triton X-100 at RT for 24 h. Photographs show the appearance of lipogels after Triton X-100, WB or 37 °C treatments. Scale bar = 5 mm. (B) Lipogels containing the indicated doses of HGNP or not containing HGNP (–) were irradiated with NIR laser operating at 44 mW mm<sup>-2</sup> for 10 min and further incubated at 37 °C/5% CO<sub>2</sub> for 50 min (NIR), or subjected to WB or 37 °C treatments for 1 h. Upper graph: DOX release in culture media. Lower graph: viability of HeLa cells seeded at a density of 5 × 10<sup>4</sup> cells cm<sup>-2</sup> and cultured for 24 h in the medium conditioned by treated lipogels. Mean and SD values are relative to the highest mean value in each panel (in panel A: (–)/Triton X-100 sample; in panel B: (–)/WB sample for upper graph and (–)/37 °C sample for lower graph), which was given an arbitrary value of 100. \*: p < 0.05 compared to 37 °C sample.

together, these results demonstrate that incorporation of Ch in LTSL-DOX formulation increased the stringency and efficiency of the delivery system based on NIR-responsive lipogels.

Furthermore, in order to increase the biocompatibility of NIR-responsive lipogels, we replaced non-metabolizable HGNP by CuSNP, which are efficient NIR-NT that can be degraded and excreted *in vivo* [39]. Recent data obtained by our group demonstrated that degradation of CuSNP also occurs when these NPs are integrated as a structural part of fibrin matrices (unpublished data). Fig. 7A shows a TEM image of a fibrin network loaded with both LTSL-DOX and CuSNP after the *in situ* polymerization of fibrinogen. Thermographic analysis of lipogels containing CuSNP in a concentration range between 0.01 and 0.05 mg mL<sup>-1</sup> revealed a

temperature increase on lipogels surface that ranged from  $3.5 \pm 0.4$  to  $21.5 \pm 0.9$  °C at the site where the laser-beam was focused for 5 min (Fig. 7B). As observed for HGNP-filled lipogels, the capacity of CuSNP-filled hydrogels to transduce NIR energy into heat was a function of the concentration of CuSNP. Irradiation of lipogels containing 0.02–0.05 mg mL<sup>-1</sup> CuSNP resulted in the discharge of DOX from regions concentric to the site where the laser beam was focused. The sizes of these regions increased with the concentration of NIR-NT (Table 1). A direct comparison of the photothermal behavior of lipogels loaded with either HGNP or CuSNP is depicted in Fig. 7C. Lipogels loaded with HGNP were more efficient in transducing NIR energy of different intensities into heat than lipogels embedding CuSNP. As observed for HGNP-loaded

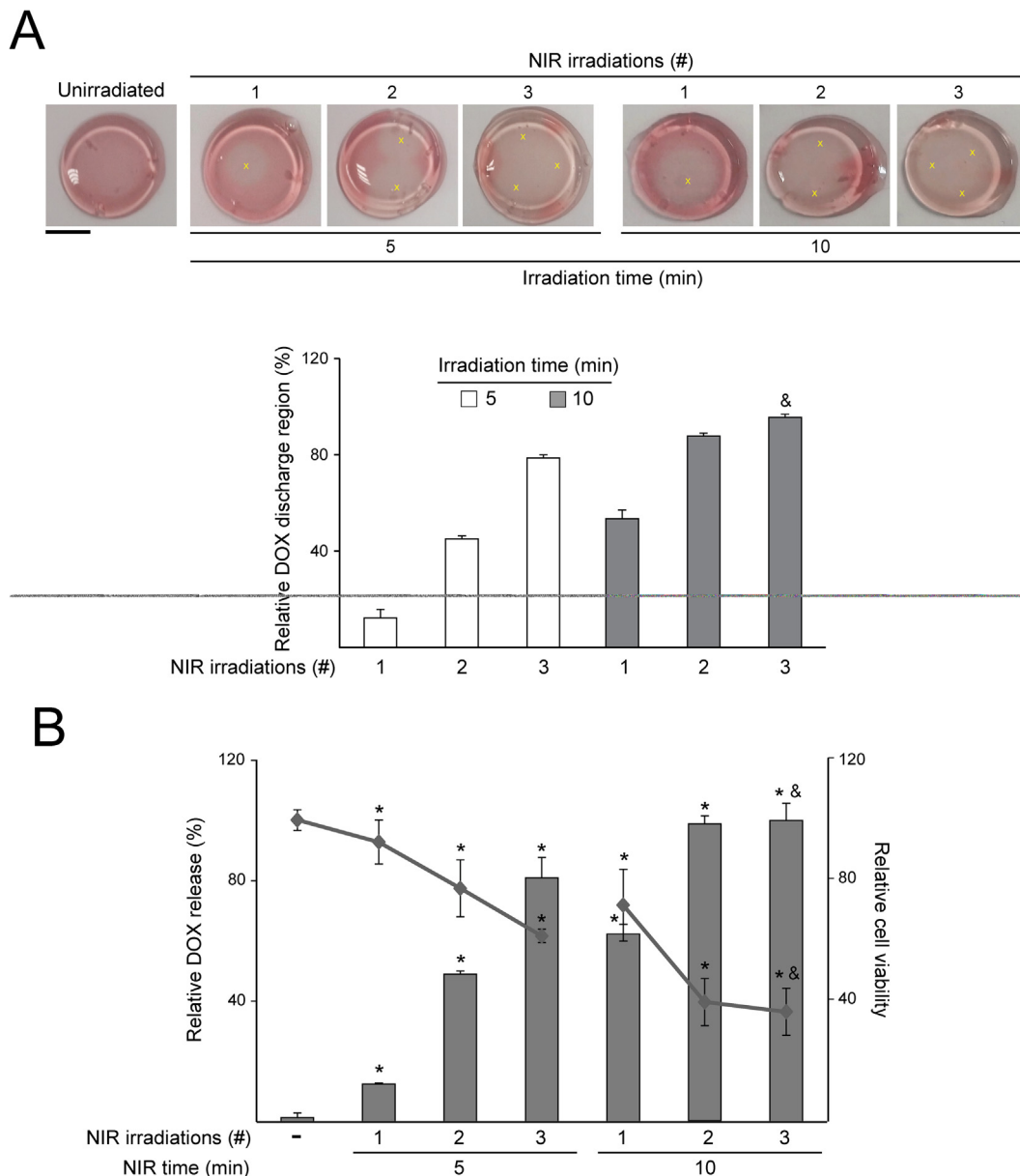


**Fig. 5.** Control over amounts of drug release from NIR-responsive lipogels. (A) Lipogels containing 0.02 mg mL<sup>-1</sup> HGNP were irradiated with NIR laser at 1–3 discrete locations, for the indicated time per location, and further incubated at 37 °C/5% CO<sub>2</sub> up to 1 h. Unirradiated samples were incubated at 37 °C/5% CO<sub>2</sub> for 1 h. Photographs show a representative set of NIR-responsive lipogels at the end of treatments. Crossmarks in photographs indicate the location where the laser beam was focused on lipogel surface. Scale bar = 1 cm. Graph: quantification of the DOX discharge area after illumination of the lipogel. (B) Histogram: DOX release in culture media conditioned by NIR-treated lipogels. Chart shows viability of HeLa cells seeded at a density of  $1 \times 10^5$  cells cm<sup>-2</sup> and incubated for 24 h in culture media containing 10% of media conditioned by NIR-treated lipogels. Mean and SD values are relative to the highest mean value in each panel (in panel A: sample NIR-irradiated at 3 locations for 10 min; in panel B: sample NIR-irradiated at 3 locations for 10 min for DOX release data, unirradiated sample for cell viability data), which was given an arbitrary value of 100. \*:  $p < 0.05$  compared to unirradiated sample. &:  $p < 0.05$  compared to condition of 2 serial NIR-irradiations for 10 min each.



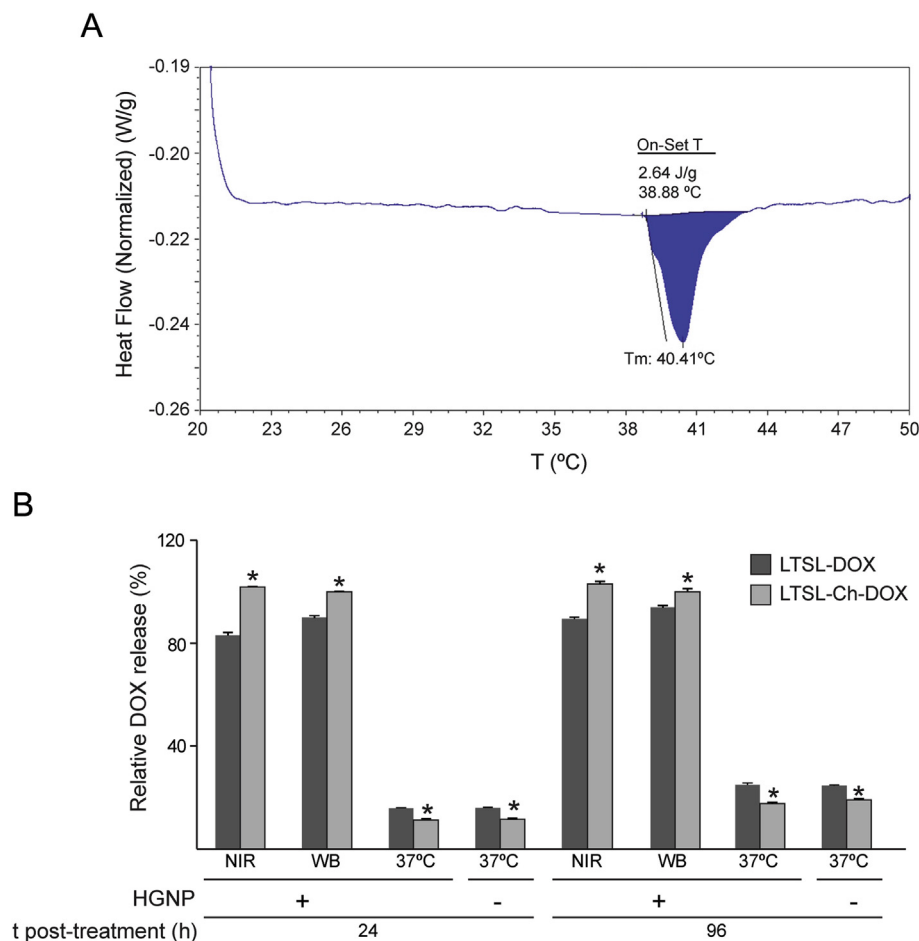


**Fig. 6.** NIR-responsive lipogels based in LTSL-Ch-DOX. (A) DSC analysis of LTSL-Ch-DOX. (B) DOX release in culture media. Lipogels, encapsulating LTSL-DOX or LTSL-Ch-DOX and containing  $0.03 \text{ mg mL}^{-1}$  HGPNP or not containing HGPNP (–) were irradiated with NIR laser operating at  $44 \text{ mW m}^{-2}$  for 10 min (NIR) or immersed in a water bath (WB) at  $42^\circ\text{C}$  for 1 h and further incubated at  $37^\circ\text{C}/5\% \text{ CO}_2$  ( $37^\circ\text{C}$ ) for 24 or 96 h. Samples not exposed to NIR or WB treatment were incubated at  $37^\circ\text{C}$  for 24 or 96 h. For each incubation time, mean and SD values are relative to DOX release data of LTSL-Ch-DOX lipogels subjected to WB treatment, which was given an arbitrary value of 100. \*:  $p < 0.05$  compared to LTSL-DOX lipogels.

lipogels, serial NIR-irradiation at discrete locations of CuSNP-loaded lipogels could be used to modulate the extent of DOX release. The media conditioned by NIR-irradiated lipogels containing CuSNP also impaired the viability of HeLa cells, demonstrating effective DOX release.

#### 4. Discussion

Methods for delivering therapeutic agents at a controlled rate and in a targeted manner have been pursued vigorously in the last decade. In this regard, much research has been focused on the development of stimuli-responsive hydrogels. Such systems consist of three-dimensional networks of crosslinked hydrophilic polymers of which the physical properties, e.g. a dramatic volume transition, are able to change abruptly in response to environmental stimuli such as pH, chemicals, electric or magnetic fields, temperature, shear stress or ultrasound [41,42]. Based on this concept, we have developed NIR-responsive lipogels as multi-component systems that provide on-demand, NIR-triggered drug release. Each component of the developed delivery system has a specific role: LTSL carry the drug to be delivered, DOX, and prevent its premature release; NIR-responsive NPs, HGPNP or CuSNP, transduce locally applied NIR energy into heat; and fibrin, deployed as a matrix that maintains both NPs in close proximity to each other in a relatively constrained location targetable by a NIR laser.

We demonstrate that simultaneous incorporation of NIR-NT and LTSL-DOX during the gelation process of fibrinogen results in the generation of hydrogels which immobilize the liposomal component and efficiently transduce NIR energy into heat. Liposomal formulation loaded in NIR-responsive lipogels consisted of DPPC as the host lipid; MSPC, a component that induce thermally-enhanced permeability to small molecules; and DSPE-PEG2000, which provides interfacial stabilizing effect [43] and brings additional steric stability to the lysolipid-induced membrane permeabilization itself, facilitating ultrafast drug release [44]. In aqueous solution, LTSL-DOX have a melting temperature of  $40.5^\circ\text{C}$  and release 50% of their cargo after water bath heating at  $42^\circ\text{C}$  for 60 s. This response to thermal challenge, similar to that shown by LTSL-DOX formulations incorporating 1-Palmitoyl-2-hydroxy-*sn*-glycero-3-phosphocholine (MPPC) [18,45], contrasts with the slow release achieved by traditional temperature-sensitive liposome formulations that incorporate hydrogenated soy phosphatidylcholine, which require 30 min of heating at  $42^\circ\text{C}$  to release 40% of loaded DOX [18]. Encapsulation of LTSL-DOX within a fibrin matrix reduced significantly their capacity to release DOX in response to a thermal challenge. Irrespectively of the concentration of NIR-NT entrapped in the fibrin matrix, lipogels released 30% of the total amount of DOX contained after 1 h at  $42^\circ\text{C}$ . Distinct from the widespread drug discharge experienced by lipogels subjected to a non-focused heating source, deposition of NIR energy for a few minutes at a discrete location of

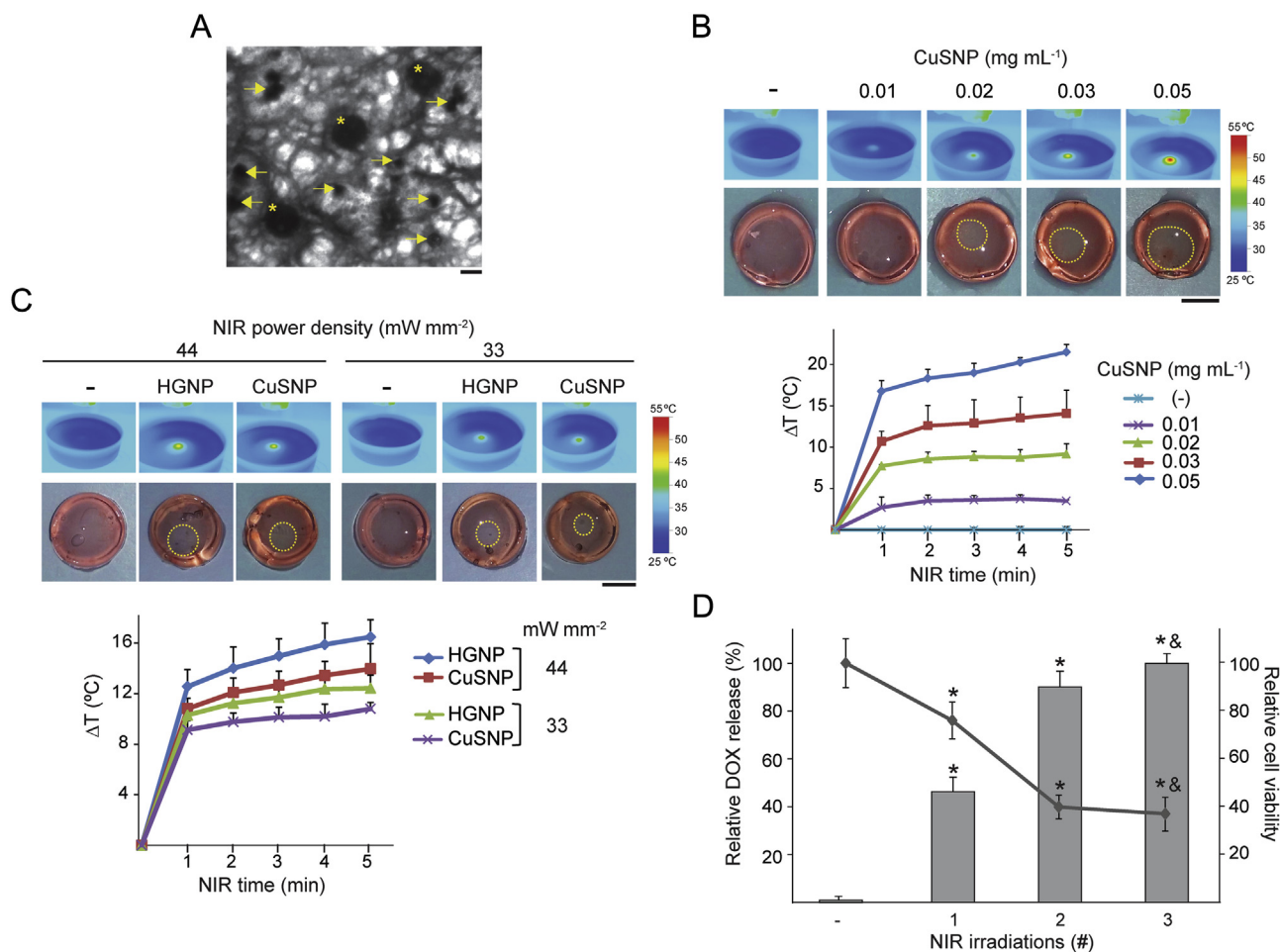


**Fig. 7.** NIR-responsive lipogels incorporating CuSNP. (A) TEM image of LTSL-DOX embedded in a fibrin matrix containing  $0.02 \text{ mg mL}^{-1}$  CuSNP. Asterisks indicate LTSL-DOX, arrows indicate CuSNP. (B–C) Lipogels prepared with LTSL-DOX and containing the indicated doses of CuSNP or not containing CuSNP (–), were irradiated with NIR laser operating at  $44 \text{ mW mm}^{-2}$  for 5 min (B). Lipogels prepared with LTSL-DOX containing  $0.02 \text{ mg mL}^{-1}$  HGNP or CuSNP, or not containing NPs (–), were irradiated with the indicated NIR laser power density for 5 min (C). NIR irradiation was monitored by IR thermography. Photographs of lipogels were obtained at the end of NIR treatment. Dashed circles indicate the region of lipogels where DOX was discharged. The lower graphs show the maximum temperature rise detected during NIR irradiation. (D) DOX release in media conditioned by lipogels treated with the indicated number of irradiations for 10 minutes each. Chart shows viability of HeLa cells seeded at a density of  $1 \times 10^5 \text{ cells cm}^{-2}$  and incubated for 24 h in culture media containing 10% of media conditioned by NIR-treated lipogels. Mean and SD values are relative to the highest mean value in the panel (sample NIR-irradiated at 3 locations for DOX release, unirradiated sample for cell viability data), which was given an arbitrary value of 100. Scale bar = 100 nm (TEM image), 5 mm (photographs). \*:  $p < 0.05$  compared to unirradiated sample. &:  $p < 0.05$  compared to condition of 2 serial NIR-irradiations.

NIR-responsive lipogels results in a rapid drug discharge in the region concentric to the laser focal point.

In order to assess the bioactivity of the released drug, HeLa cells were exposed to the media conditioned by illuminated lipogels. Single irradiation ( $44 \text{ mW mm}^{-2}$  for 10 min) of lipogels containing  $0.03 \text{ mg mL}^{-1}$  HGNP led to the release of an amount of DOX that reduced about ten times the metabolic activity of cancer cells. Bioactivity of the liposomal cargo was not adversely affected by the laser triggering as similar cytotoxic activity was detected in media from lipogels lacking NIR-NT and incubated for 1 h at  $42^\circ\text{C}$ .

Different heating profiles can be achieved through the modulation of the concentration of NIR-NT incorporated within the fibrin matrix or the intensity of deposited NIR energy, allowing fine regulation of drug release from NIR-responsive lipogels. The number of irradiations and their respective duration could be used to precisely define the final concentration of released drug, and therefore, the level of bioactivity of the lipogel cargo on the targeted cell population. Moreover, sequential irradiation of the composites at overlapping spatial locations allows tight control over DOX release without disturbing the structure of the hydrogel network.

Drug release rates have important implications for therapeutic activities of any drug delivery system. The drug dosage needs to reach certain values to be effective within its therapeutic window, minimizing the risk of toxic side effects outside the site in the need of therapy. Triggerable drug delivery system presented in this paper, built on the unique properties of fibrin such as injectability and biodegradability, circumvents many of the problems associated with the use of circulating liposomes to control local bioavailable drug concentrations (e.g. potential clearance by the mononuclear phagocyte system (MPS) which can lead to toxicity in MPS organs; vesicular degradation, aggregation or fusion events that compromise liposomal stability at the desired target site [46–49]). It is well known that bilayer-tightening conducted by Ch in liposomal formulations increases the retention of cargos into lipid vesicles [50–53]. The incorporation of LTSL-Ch-DOX within NIR-responsive fibrin matrices improved significantly the efficiency of the delivery system. Ch does not only reduce the cargo leakage observed at  $37^\circ\text{C}$  but also increases the total amount of released drug after thermal treatment. This refinement was achieved without compromising the long-term stability of the lipogel formulation. The incorporation of CuSNP as NIR-NT in the lipogels adds

safety to the drug delivery platform and may facilitate its translation to clinical applications. Copper, essential for human health [54], has a highest safe intake level of 10 mg daily in adults [55]. Recent preclinical studies demonstrated that biodegradability of pegylated CuSNP is distinct to non-metabolizable pegylated HGNP after systemic administration, revealing that their low long-term nanotoxicity is tightly related to their dynamics of disintegration *in vivo* and their ability of being eliminated efficiently through both hepatobiliary and renal excretion [39].

Integration of liposomal technology, the first drug delivery system approved for clinical purposes, within “smart” hydrogels responsive to NIR-light adds a remarkable advantage to composite systems based on the combination of liposomes and degradable polymeric materials for the delivery of different bioactive molecules [56]. NIR-responsive lipogels technology may overcome composite systems that mostly depend on degradation of polymeric materials, which in many cases leads to insufficient initial release at commencement of treatment or high overdose during the fast degradation period [57].

NIR-responsive lipogels technology is well-suited to reach the clinical scenario. The mixture of fibrinogen, thrombin, liposomes and NIR-NT can be polymerized *in situ* into virtually any anatomical region by imaging-guided intratissue injection or infusion using catheterization. Moreover, intraoperative implantation of polymerized lipogels may be also a choice to place NIR-responsive lipogels at the target site. Penetration shown by NIR laser light through biological tissues allows reaching depths of at least 10 cm in breast tissue and 4 cm of skull/brain tissue or deep muscle using micro-watt laser sources; and up to 7 cm of muscle and neonatal skull/brain when using high power laser sources [58]. Alternatively, needle probes can be used to drive an optical fiber that delivers NIR energy at the target site, as in the minimally invasive procedure termed “interstitial laser therapy”, currently used in a clinical trial for ablation of prostate tissue [59]. There are a variety of technological resources currently available in the marketplace to adapt NIR energy deposition to the size and shape of the target, allowing several applications in one session. Technical operative conditions that may ensure an efficient laser application on implanted NIR-responsive lipogels include irradiation time, power density control and even dispersion of NIR-light through the use of light distributors, diffusers or laser arrays which can also define the geometry of the irradiated areas. Finally, easy handling and high safety standards of NIR lasers are critical factors that may pave the way of NIR-responsive lipogels technology to the clinical setting.

## 5. Conclusions

The *in situ* polymerization of fibrinogen allows the simultaneous encapsulation of different LTSL formulations and NIR-NT within fibrin networks. The resulting lipogels efficiently transform NIR energy into heat. The rise of local temperature above the transition temperature of the entrapped liposomes promotes DOX release from the lipogel regions concentric to the irradiation site. This effect leads to the increase of drug levels in the media conditioned by NIR-responsive composites. DOX release from NIR-responsive lipogels can be finely modulated by the amount of embedded NIR-NT, the intensity of NIR energy deposited or the irradiation regime. Incorporation of Ch in LTSL-DOX formulations results in a significant reduction of the cargo leakiness in lipogels maintained at normal human body temperature, increasing the effectiveness of the on-demand drug delivery platform. Finally, the compatibility of biodegradable NIR-NT with the developed system together with the use of resorbable polymeric matrices and NIR-light, comply with safety standards for future clinical use.

## Disclosure

The authors declare no competing financial interest.

## Acknowledgements

The authors thank to D. Morales (Confocal Microscopy Laboratory, Universidad Autónoma de Madrid, Spain (UAM)) as well as F. Urbano and C. Aguado (Transmission Electron Microscopy Laboratory, UAM) for excellent technical support. This work was supported by grant PI15/01118 from the Instituto de Salud Carlos III-Fondos FEDER, Ministry of Economy and Competitiveness, Spain (MINECO); grant SAF2013-50364-EXP from MINECO; grant S2013/MIT-2862 from Comunidad Autónoma de Madrid, Spain (CAM) and grant Roche-IdiPAZ from the intramural funding program of Foundation for Biomedical Research of La Paz University Hospital-IdiPAZ. ER-H acknowledges the School of Pharmacy and Pharmaceutical Sciences, Trinity College Dublin, for Ussher start-up funding. NV is supported by Program I2 from CAM.

## Appendix A. Supplementary data

Supplementary data associated with this article can be found, in the online version, at <http://dx.doi.org/10.1016/j.actbio.2017.08.010>.

## References

- [1] E. Ahmad, M.T. Fatima, M. Hoque, M. Owais, M. Saleemuddin, Fibrin matrices: the versatile therapeutic delivery systems, *Int. J. Biol. Macromol.* 81 (2015) 121–136.
- [2] Y. Li, H. Meng, Y. Liu, B.P. Lee, Fibrin gel as an injectable biodegradable scaffold and cell carrier for tissue engineering, *Sci. World J.* 2015 (2015) 685690.
- [3] T. Vermonden, R. Censi, W.E. Hennink, Hydrogels for protein delivery, *Chem. Rev.* 112 (5) (2012) 2853–2888.
- [4] G. Wozniak, Fibrin sealants in supporting surgical techniques: the importance of individual components, *Cardiovasc. Surg.* 11 (Suppl 1) (2003) 17–21.
- [5] T. Osathanon, C.M. Giachelli, M.J. Somerman, Immobilization of alkaline phosphatase on microporous nanofibrous fibrin scaffolds for bone tissue engineering, *Biomaterials* 30 (27) (2009) 4513–4521.
- [6] K.M. Lorentz, S. Kontos, P. Frey, J.A. Hubbell, Engineered aprotinin for improved stability of fibrin biomaterials, *Biomaterials* 32 (2) (2011) 430–438.
- [7] T.W. Chung, M.C. Yang, W.J. Tsai, A fibrin encapsulated liposomes-in-chitosan matrix (FLCM) for delivering water-soluble drugs. Influences of the surface properties of liposomes and the crosslinked fibrin network, *Int. J. Pharm.* 311 (1–2) (2006) 122–129.
- [8] S.S. Wang, M.C. Yang, T.W. Chung, Liposomes/chitosan scaffold/human fibrin gel composite systems for delivering hydrophilic drugs—release behaviors of tirofiban *in vitro*, *Drug Deliv.* 15 (3) (2008) 149–157.
- [9] T.M. Allen, C. Hansen, F. Martin, C. Redemann, A. Yau-Young, Liposomes containing synthetic lipid derivatives of poly(ethylene glycol) show prolonged circulation half-lives *in vivo*, *Biochim. Biophys. Acta* 1066 (1) (1991) 29–36.
- [10] H. Takeuchi, H. Kojima, H. Yamamoto, Y. Kawashima, Evaluation of circulation profiles of liposomes coated with hydrophilic polymers having different molecular weights in rats, *J. Controlled Release* 75 (1–2) (2001) 83–91.
- [11] K. Moribe, K. Maruyama, M. Iwatsuru, Molecular localization and state of amphotericin B in PEG liposomes, *Int. J. Pharm.* 193 (1) (1999) 97–106.
- [12] M.J. Johnston, S.C. Semple, S.K. Klimuk, K. Edwards, M.L. Eisenhardt, E.C. Leng, G. Karlsson, D. Yanko, P.R. Cullis, Therapeutically optimized rates of drug release can be achieved by varying the drug-to-lipid ratio in liposomal vincristine formulations, *Biochim. Biophys. Acta* 1758 (1) (2006) 55–64.
- [13] K.M. Laginha, S. Verwoert, G.J. Charrois, T.M. Allen, Determination of doxorubicin levels in whole tumor and tumor nuclei in murine breast cancer tumors, *Clin. Cancer Res.* 11 (19 Pt 1) (2005) 6944–6949.
- [14] A.M. Ponce, Z. Vujaskovic, F. Yuan, D. Needham, M.W. Dewhirst, Hyperthermia mediated liposomal drug delivery, *Int. J. Hyperthermia* 22 (3) (2006) 205–213.
- [15] A. Puri, K. Loomis, B. Smith, J.H. Lee, A. Yavlovich, E. Heldman, R. Blumenthal, Lipid-based nanoparticles as pharmaceutical drug carriers: from concepts to clinic, *Crit. Rev. Ther. Drug Carrier Syst.* 26 (6) (2009) 523–580.
- [16] S. Bibi, E. Lattmann, A.R. Mohammed, Y. Perrie, Trigger release liposome systems: local and remote controlled delivery?, *J. Microencapsulation* 29 (3) (2012) 262–276.
- [17] B. Du, S. Han, H. Li, F. Zhao, X. Su, X. Cao, Z. Zhang, Multi-functional liposomes showing radiofrequency-triggered release and magnetic resonance imaging for tumor multi-mechanism therapy, *Nanoscale* 7 (12) (2015) 5411–5426.

- [18] D. Needham, G. Anyarambhatla, G. Kong, M.W. Dewhirst, A new temperature-sensitive liposome for use with mild hyperthermia: characterization and testing in a human tumor xenograft model, *Cancer Res.* 60 (5) (2000) 1197–1201.
- [19] B. Banno, L.M. Ickenstein, G.N. Chiu, M.B. Bally, J. Thewalt, E. Brief, E.K. Wasan, The functional roles of poly(ethylene glycol)-lipid and lysolipid in the drug retention and release from lysolipid-containing thermosensitive liposomes in vitro and in vivo, *J. Pharm. Sci.* 99 (5) (2010) 2295–2308.
- [20] H. Grull, S. Langereis, Hyperthermia-triggered drug delivery from temperature-sensitive liposomes using MRI-guided high intensity focused ultrasound, *J. Controlled Release* 161 (2) (2012) 317–327.
- [21] A. López-Noriega, E. Ruiz-Hernández, E. Quinlan, G. Storm, W.E. Hennink, F.J. O'Brien, Thermally triggered release of a pro-osteogenic peptide from a functionalized collagen-based scaffold using thermosensitive liposomes, *J. Controlled Release* 187 (2014) 158–166.
- [22] M. van Elk, B.P. Murphy, T. Eufrazio-da-Silva, D.P. O'Reilly, T. Vermonden, W.E. Hennink, G.P. Duffy, E. Ruiz-Hernandez, Nanomedicines for advanced cancer treatments: transitioning towards responsive systems, *Int. J. Pharm.* 515 (1–2) (2016) 132–164.
- [23] Y. Dou, K. Hynynen, C. Allen, To heat or not to heat: challenges with clinical translation of thermosensitive liposomes, *J. Controlled Release* 249 (2017) 63–73.
- [24] Celsion Corporation. Study of ThermoDox™ With Standardized Radiofrequency Ablation (RFA) for Treatment of Hepatocellular Carcinoma (HCC) (OPTIMA). In: ClinicalTrials.gov [Internet]. Bethesda (MD): National Library of Medicine (US). 2000-[cited 2017 1 March]. Available from: <https://clinicaltrials.gov/ct2/show/NCT02112656> NLM identifier: NCT00004451.
- [25] Celsion Corporation. A Study of ThermoDox™ in Combination With Radiofrequency Ablation (RFA) in Primary and Metastatic Tumors of the Liver (HEAT). In: ClinicalTrials.gov [Internet]. Bethesda (MD): National Library of Medicine (US). 2000-[cited 2017 1 March]. Available from: <https://clinicaltrials.gov/ct2/show/NCT00441376> NLM identifier: NCT00441376.
- [26] V. Cebrian, F. Martín-Saavedra, L. Gomez, M. Arruebo, J. Santamaria, N. Vilaboa, Enhancing of plasmonic photothermal therapy through heat-inducible transgene activity, *Nanomedicine* 9 (5) (2013) 646–656.
- [27] Y. Li, W. Lu, Q. Huang, M. Huang, C. Li, W. Chen, Copper sulfide nanoparticles for photothermal ablation of tumor cells, *Nanomedicine (Lond)* 5 (8) (2010) 1161–1171.
- [28] F.M. Martín-Saavedra, V. Cebrian, L. Gomez, D. Lopez, M. Arruebo, C.G. Wilson, R.T. Franceschi, R. Voellmy, J. Santamaria, N. Vilaboa, Temporal and spatial patterning of transgene expression by near-infrared irradiation, *Biomaterials* 35 (28) (2014) 8134–8143.
- [29] B.E. Smith, P.B. Roder, X. Zhou, P.J. Pauzauskie, Nanoscale materials for hyperthermal theranostics, *Nanoscale* 7 (16) (2015) 7115–7126.
- [30] H.S. O'Neill, C.C. Herron, C.L. Hastings, R. Deckers, A. Lopez Noriega, H.M. Kelly, W.E. Hennink, C.O. McDonnell, F.J. O'Brien, E. Ruiz-Hernández, G.P. Duffy, A stimuli responsive liposome loaded hydrogel provides flexible on-demand release of therapeutic agents, *Acta Biomater.* 48 (2017) 110–119.
- [31] A. Lopez-Noriega, C.L. Hastings, B. Ozbakir, K.E. O'Donnell, F.J. O'Brien, G. Storm, W.E. Hennink, G.P. Duffy, E. Ruiz-Hernandez, Hyperthermia-induced drug delivery from thermosensitive liposomes encapsulated in an injectable hydrogel for local chemotherapy, *Adv. Healthcare Mater.* 3 (6) (2014) 854–859.
- [32] A. Fritze, F. Hens, A. Kimpfler, R. Schubert, R. Peschka-Suss, Remote loading of doxorubicin into liposomes driven by a transmembrane phosphate gradient, *Biochim. Biophys. Acta* 1758 (10) (2006) 1633–1640.
- [33] G. Haran, R. Cohen, L.K. Bar, Y. Barenholz, Transmembrane ammonium sulfate gradients in liposomes produce efficient and stable entrapment of amphipathic weak bases, *Biochim. Biophys. Acta, Biomembr.* 1151 (2) (1993) 201–215.
- [34] K.K. Karukstis, E.H. Thompson, J.A. Whiles, R.J. Rosenfeld, Deciphering the fluorescence signature of daunomycin and doxorubicin, *Biophys. Chem.* 73 (3) (1998) 249–263.
- [35] T. Higuchi, Mechanism of sustained-action medication theoretical analysis of rate of release of solid drugs dispersed in solid matrices, *J. Pharm. Sci.* 52 (1963) 1145–1149.
- [36] J. Schindelin, I. Arganda-Carreras, E. Frise, V. Kaynig, M. Longair, T. Pietzsch, S. Preibisch, C. Rueden, S. Saalfeld, B. Schmid, J.Y. Tinevez, D.J. White, H. Hartenstein, K. Eliceiri, P. Tomancak, A. Cardona, Fiji: an open-source platform for biological-image analysis, *Nat. Methods* 9 (7) (2012) 676–682.
- [37] X. Li, D.J. Hirsh, D. Cabral-Lilly, A. Zirkel, S.M. Gruner, A.S. Janoff, W.R. Perkins, Doxorubicin physical state in solution and inside liposomes loaded via a pH gradient, *Biochim. Biophys. Acta* 1415 (1) (1998) 23–40.
- [38] P.J. Gaillard, C.C.M. Appeldoorn, R. Dorland, J. van Kregten, F. Manca, D.J. Vugts, B. Windhorst, G. van Dongen, H.E. de Vries, D. Maussang, O. van Tellingen, Pharmacokinetics, brain delivery, and efficacy in brain tumor-bearing mice of glutathione pegylated liposomal doxorubicin (2B3-101), *Plos One* 9 (1) (2014).
- [39] L. Guo, I. Panderi, D.D. Yan, K. Szulak, Y. Li, Y.T. Chen, H. Ma, D.B. Niesen, N. Seeram, A. Ahmed, B. Yan, D. Pantazatos, W. Lu, A comparative study of hollow copper sulfide nanoparticles and hollow gold nanospheres on degradability and toxicity, *ACS Nano* 7 (10) (2013) 8780–8793.
- [40] R.A. Demel, B. De Kruffy, The function of sterols in membranes, *Biochim. Biophys. Acta* 457 (2) (1976) 109–132.
- [41] R.M. Ottenbrite, K. Park, T. Okano, *Biomedical Applications of Hydrogels Handbook*, 1st ed., Springer, New York, 2010.
- [42] M.C. Koetting, J.T. Peters, S.D. Steichen, N.A. Peppas, Stimulus-responsive hydrogels: theory, modern advances, and applications, *Mater. Sci. Eng., R* 93 (2015) 1–49.
- [43] D. Papahadjopoulos, K. Jacobson, S. Nir, T. Isac, Phase transitions in phospholipid vesicles. Fluorescence polarization and permeability measurements concerning the effect of temperature and cholesterol, *Biochim. Biophys. Acta* 311 (3) (1973) 330–348.
- [44] D. Needham, J.Y. Park, A.M. Wright, J. Tong, Materials characterization of the low temperature sensitive liposome (LTSL): effects of the lipid composition (lysolipid and DSPE-PEG2000) on the thermal transition and release of doxorubicin, *Faraday Discussions* 161 (2013) 515–534; discussion 563–89.
- [45] M.H. Gaber, N.Z. Wu, K. Hong, S.K. Huang, M.W. Dewhirst, D. Papahadjopoulos, Thermosensitive liposomes: extravasation and release of contents in tumor microvascular networks, *Int. J. Radiat. Oncol. Biol. Phys.* 36 (5) (1996) 1177–1187.
- [46] T.M. Allen, P.R. Cullis, Liposomal drug delivery systems: from concept to clinical applications, *Adv. Drug Deliv. Rev.* 65 (1) (2013) 36–48.
- [47] G. Storm, H.J. Van Gessel, P.A. Steerenberg, P.A. Speth, F.H. Roerdink, J. Regts, M. Van Veen, W.H. De Jong, Investigation of the role of mononuclear phagocytes in the transportation of doxorubicin-containing liposomes into a solid tumor, *Cancer Drug Deliv.* 4 (2) (1987) 89–104.
- [48] L. Zhang, S. Granick, How to stabilize phospholipid liposomes (using nanoparticles), *Nano Lett.* 6 (4) (2006) 694–698.
- [49] N. Grimaldi, F. Andrade, N. Segovia, L. Ferrer-Tasies, S. Sala, J. Veciana, N. Ventosa, Lipid-based nanovesicles for nanomedicine, *Chem. Soc. Rev.* 45 (23) (2016) 6520–6545.
- [50] G. Storm, F.H. Roerdink, P.A. Steerenberg, W.H. de Jong, D.J. Crommelin, Influence of lipid composition on the antitumor activity exerted by doxorubicin-containing liposomes in a rat solid tumor model, *Cancer Res.* 47 (13) (1987) 3366–3372.
- [51] T.J. McIntosh, The effect of cholesterol on the structure of phosphatidylcholine bilayers, *Biochim. Biophys. Acta* 513 (1) (1978) 43–58.
- [52] P.R. Cullis, M.J. Hope, The bilayer stabilizing role of sphingomyelin in the presence of cholesterol: a 31P NMR study, *Biochim. Biophys. Acta* 597 (3) (1980) 533–542.
- [53] J. Damen, J. Regts, G. Scherphof, Transfer and exchange of phospholipid between small unilamellar liposomes and rat plasma high density lipoproteins. Dependence on cholesterol content and phospholipid composition, *Biochim. Biophys. Acta* 665 (3) (1981) 538–545.
- [54] J.Y. Uriu-Adams, C.L. Keen, Copper, oxidative stress, and human health, *Mol. Aspects Med.* 26 (4–5) (2005) 268–298.
- [55] I.o.M.U.P.o. Micronutrients, Dietary Reference Intakes for Vitamin A, Vitamin K, Arsenic, Boron, Chromium, Copper, Iodine, Iron, Manganese, Molybdenum, Nickel, Silicon, Vanadium, and Zinc, National Academies Press (US), Washington (DC), 2001.
- [56] M.S. Mufamadi, V. Pillay, Y.E. Choonara, L.C. Du Toit, G. Modi, D. Naidoo, V.M. Ndesendo, A review on composite liposomal technologies for specialized drug delivery, *J. Drug Deliv.* 2011 (2011) 939851.
- [57] W.B. Liechty, D.R. Kryscio, B.V. Slaughter, N.A. Peppas, Polymers for drug delivery systems, *Annu. Rev. Chem. Biomol. Eng.* 1 (2010) 149–173.
- [58] R. Weissleder, A clearer vision for in vivo imaging, *Nat. Biotechnol.* 19 (4) (2001) 316–317.
- [59] J.M. Stern, V.V. Kibanov Solomonov, E. Sazykina, J.A. Schwartz, S.C. Gad, G.P. Goodrich, Initial evaluation of the safety of nanoshell-directed photothermal therapy in the treatment of prostate disease, *Int. J. Toxicol.* 35 (1) (2016) 38–46.